Sensor-Free Biosensing of Mitral and Aortic Valvular Function During Continuous Flow Left Ventricular Assist Device Support

Link to publication record in Ulster University Research Portal

Document Version
Author Accepted version

Sensor-Free Biosensing of Mitral and Aortic Valvular Function During Continuous Flow Left Ventricular Assist Device Support

Selim Bozkurt*, and Nikhil Bhalla*

Abstract— Objective: **Continuous Flow Left Ventricular Assist Devices (CF-LVADs) are miniaturised devices supporting the failing left ventricle and alter the blood flow in the cardiovascular system which may cause severe health complications. Regurgitation and stenosis in mitral and aortic valves may further aggravate complications and limit the efficiency of CF-LVAD support. Within this context, real-time monitoring of the blood flow in the CF-LVAD support will allow early detection of mitral and aortic valve problems and timely intervention before the valvular problems are worsened. Addressing these issues, this study detects mitral regurgitation, stenosis, and aortic regurgitation during CF-LVAD support by monitoring CF-LVAD electrical current.** *Methods:* **Patient-specific electrocardiograph RR interval time series with normal sinus rhythm were incorporated into a cardiovascular system model including CF-LVAD whilst simulating mild and moderate mitral regurgitation, stenosis, and aortic regurgitation. Spearman rank test was used to analyse the correlation between CF-LVAD electrical current signal waveforms over left ventricular systole and left atrial contraction.** *Results:* **Correlation coefficients between the CF-LVAD electrical current signals in normal heart valve function and mild and moderate mitral regurgitation were 0.07 and -0.68. In normal heart valve function and mild and moderate mitral stenosis were 0.82 and 0.68. Within the normal heart valve function and mild and moderate aortic regurgitation the correlation coefficients 0.86 and 0.61, respectively.** *Conclusion:* **These results suggest that CF-LVAD electrical current signal waveforms can be used for both diagnosis and prognosis of mitral and aortic disorders, thereby representing a potential innovation in the field of both bioelectronics and biosensors.**

Index Terms—**mitral regurgitation, mitral stenosis, aortic regurgitation, CF-LVAD, sensor free biosensing**

I. INTRODUCTION

CONTINUOUS Flow Left Ventricular Assist Devices (CF-LVADs) are miniaturised devices supporting failing left ventricle [1] and alter the blood flow in cardiovascular system which may cause complications [2]. Problems in mitral and aortic valves such as regurgitation and stenosis may cause further complications which limit the efficiency of CF-LVAD support [3] [4]. Prolapsed mitral leaflets, ruptured chordae tendineae or clefts in the mitral valve may cause primary mitral regurgitation after CF-LVAD support [4]. Although

intervention to correct the mitral valve is not suggested unless ventricular recovery occurs, additional complications due to mitral regurgitation increase morbidity in patients implanted with a CF-LVAD [4]. For instance, pulmonary hypertension is associated with left ventricular dysfunction, and it may be worsened with the reverse blood flow through the mitral valve [5]. It is also reported that increased pulmonary arterial pressure affects heart transplant suitability negatively [6]. The right ventricular function is worsened in patients with residual mitral regurgitation, and it is associated with postoperative bleeding and multiorgan failure [7] whilst severely failing right ventricle may require right VAD support [8]. Also, surgical correction of the mitral valve during CF-LVAD implantation reduces readmissions and morbidities in patients supported with CF-LVAD [9]. On the other hand, the mitral stenosis affects CF-LVAD inflow thus having an impact on the pump outflow [4]. This might be attributed to the subsequent result of mitral regurgitation treatment [4]. Although pump inflow velocities are in a similar range in patients with and without mitral stenosis during CF-LVAD support [10], the source of blood acceleration may be different indicating that cause of impaired left ventricular filling is also different [10]. Aortic valve does not open fully due to continuous unloading of the left ventricle during CF-LVAD support [11]. In this case, aortic valve tissue may deteriorate due to altered load and result in reverse blood flow through the aortic valve [12]. Patients implanted with a CF-LVAD and having uncorrected mild aortic insufficiency have a higher risk of developing moderate or severe aortic regurgitation [13] which reduces the efficiency of CF-LVAD support.

Sensing changes in blood flow or pressure within the CF-LVADs will be significant improvement in these devices for long-term standard care for patients with end-stage heart failure. CF-LVAD flow rate and electrical current signal waveforms are sensitive to changes in cardiac dynamics [14]. Therefore, CF-LVAD signals have been utilised to regulate operating speed to optimise the CF-LVAD support. A sensor-free adaptive control algorithm was used to regulate CF-LVAD operating speed according to vascular resistances, volumes, and heart rate by controlling the pump flow rate [15]. A sensor-free modular multi objective control algorithm was also utilised to

*S. Bozkurt is with the Ulster University, School of Engineering, Belfast, UK (correspondence e-mail: s.bozkurt1@ulster.ac.uk). *N. Bhalla is now with Ulster University, Nanotechnology and Integrated Bioengineering Centre

(NIBEC) at School of Engineering and Ulster University, Healthcare Technology Hub, Belfast, UK (correspondence e-mail: n.bhalla@ulster.ac.uk).

control pump operating speed to adjust the level of CF-LVAD support according to physical activities [16]. The main advantages of sensor-free measurements for the physiological activity of heart, in terms of flow, over physical sensors [17], optical pressure sensors [18] and other sensing systems [19], [20] is that it avoids incorporation of an additional components within a device. This reduces the complexity associated with implantation of a sensor within body, thereby reducing the risk of additional complications in long-term use of CF-VAD [21].

Henceforth, in this work we detect mitral regurgitation, stenosis, and aortic regurgitation during CF-LVAD support by continuously monitoring CF-LVAD electrical current. These CF-LVAD signals have also the potential to be utilised as cardiac monitoring systems and detect complications altering blood flow in cardiovascular system during CF-LVAD support. Using our approach for the continuous monitoring of mitral and aortic valve conditions in patients will allow following the progress of valvular problems during CF-LVAD support. In addition, the early detection of mitral and aortic valve problems will allow timely intervention before the valvular problems are worsened.

II. MATERIALS AND METHODS

Clinical conditions evaluated in this study were dilated cardiomyopathy with normal heart valve functions, mild & moderate mitral and aortic regurgitations, and mild & moderate mitral stenosis during CF-LVAD support using a patient-specific electrocardiogram RR interval time series with normal sinus rhythm [22] for all the conditions. Mild and moderate mitral insufficiencies were simulated considering the criteria for regurgitant volume in primary mitral regurgitation [23]. Mild and moderate mitral stenoses were simulated considering the criteria for mean pressure gradient [24]. Mild and moderate aortic insufficiencies were simulated considering the criteria for regurgitant volume in aortic regurgitation [25]. Mild right ventricular failure was simulated considering the criteria for cardiac index and assuming a 2 m^2 body surface area in post-LVAD implantation [26].

A numerical model simulating cardiac function and blood flow rates and pressure in the cardiovascular system served as the test platform to evaluate mitral and aortic valvular physiologies during CF-LVAD support. The numerical model used in this study simulates the relation between heart chamber dimensions (i.e., long axis length and basal diameter) and pressures. Left ventricular pressure (p_{lv}), volume (V_{lv}) and change of basal radius with (dr_{lv}/dt) are described as given below.

$$p_{lv} = p_{lv,a} + p_{lv,p} \tag{1}$$

$$p_{lv,a}(t) = E_{es,lv}\left(V_{lv} - V_{lv,0}\right) f_{act,lv}(t) \tag{2}$$

$$p_{lv,p} = A\left(e^{B\left(V_{lv}-V_{lv,0}\right)} - 1\right) \tag{3}$$

$$V_{lv} = \frac{2}{3}\pi K_{lv} r_{lv}^2 l_{lv} \tag{4}$$

$$\frac{dr_{lv}}{dt} = \frac{3\left(Q_{mv} - Q_{av}\right)}{4\pi K_{lv} l_{lv}} \left(\frac{3V_{lv}}{2\pi K_{lv} l_{lv}}\right)^{-1/2} \tag{5}$$

Here, $p_{lv,a}$ and $p_{lv,p}$ represents the pressures in the left ventricle due to active contraction and filling, respectively. $E_{es,lv}$ is the elastance, $f_{act,lv}$ is the activation function driving the time-varying cardiac events, A and B are coefficients, $V_{lv,0}$ is the volume in the left ventricle at zero pressure, K_{lv} and l_{lv} is a shape parameter and long axis length, Q_{mv} and Q_{av} are the flow rates through the valves. The left atrial pressure (p_{la}) and volume (V_{la}) relationship was described using a time-varying elastance (E_{la}) model [27].

$$p_{la}(t) = E_{la}(t)\left(V_{la} - V_{la,0}\right) \tag{6}$$

$$E_{la}(t) = E_{min,la} + 0.5\left(E_{max,la} - E_{min,la}\right) f_{act.la}(t-D) \tag{7}$$

Here, $E_{min,la}$ and $E_{max,la}$ are the minimal and maximal atrial elastances over a cardiac cycle, $f_{act,la}$ is the activation function driving the time-varying cardiac events. The right ventricular pressure and volume signals were modeled in an equivalent way to the left ventricular pressure and volume signals using different parameter values. The right atrial pressure and volume signals were modeled in an identical manner to the left atrial pressure and volume signals using different parameter values. The right ventricular and atrial functions were simulated using similar equations with different parameter values.

The circulatory system includes systemic and pulmonary circulations and cerebral circulation. Blood flow rates and pressures in the circulatory system were simulated using an electric analogue model which includes resistance, inertance, and compliance elements. Detailed information about the cardiovascular system model can be found in [27], [28].

CF-LVAD model utilised in this study simulates the hydrodynamic and mechanical characteristics of an axial flow heart pump which is an optimised version of DeBakey pump [29]. Hydraulic characteristics of the CF-LVAD were simulated using a flow source term (K_1), hydraulic resistance ($R_{CF-LVAD}$), inertance ($L_{CF-LVAD}$) and operating speed of the CF-LVAD ($n_{CF-LVAD}$) [30] as given below.

$$L_{CF-LVAD}\frac{dQ_{CF-LVAD}}{dt_{CF-LVAD}} = K_1 n_{CF-LVAD}^2 - R_{CF-LVAD}Q_{CF-LVAD} - \Delta p_{CF-LVAD} \tag{8}$$

Mechanical characteristics of the CF-LVAD were simulated by modelling the electrical torque (T_e) and load torque (T_p) of the pump as described in [31] and are given below.

$$J_{CF-LVAD}\frac{dn_{CF-LVAD}}{dt_{CF-LVAD}} = T_e - (C_0 + C_v n_{CF-LVAD}) - T_p \tag{9}$$

$$T_e = k_m I_{CF-LVAD} \tag{10}$$

$$T_p = K_2 n_{CF-LVAD}^2 + K_3 n_{CF-LVAD}Q_{CF-LVAD} + K_4 Q_{CF-LVAD} \tag{11}$$

Here, $J_{CF-LVAD}$ rotor inertia, C_0 is static friction torque, C_v is the viscous damping factor of the motor, k_m is the torque constant and $I_{CF-LVAD}$ is the electrical current. K_2, K_3 and K_4 are the empirical coefficients used to describe load torque. Parameter values used in the equations describing the hydraulic and mechanical characteristics of the CF-LVAD are given in Table 1.

TABLE I
PARAMETER VALUES USED IN THE EQUATIONS DESCRIBING THE HYDRAULIC AND MECHANICAL CHARACTERISTICS OF THE CF-LVAD

CF-LVAD Parameter	Value
$J_{CF-LVAD}$ [g cm^2]	3.95
C_0 [N mm/A]	8.56
C_v [N mm/rpm]	3.75×10^{-5}
K_1 [mmHg s^2]	0.00323
K_2 [N mm s^2]	0.0017
K_3 [N mm s^2/mL]	-0.00003
K_4 [N mm s/mL]	0.00596
$R_{CF-LVAD}$ [mmHg s/mL]	0.238
$L_{CF-LVAD}$ [mmHg s^2/mL]	0.00168

J is the inertia, C_0 and C_v are the static friction torque and viscous damping factor in the motor, K_1, K_2, K_3 and K_4 are the empirically determined coefficients, $R_{CF-LVAD}$ and $L_{CF-LVAD}$ are pump resistance and inertance, respectively

Parameter values simulating CF-LVAD support with normal sinus rhythm and modified parameter values used to simulate clinical conditions in the cardiovascular system model are given in Table 2. Other parameter values used in the cardiovascular system model can be found in [27].

TABLE II
PARAMETER VALUES SIMULATING VALVULAR CONDITIONS DURING CF-LVAD SUPPORT

	$R_{mv,f}$ [mmHgs/mL]	$R_{mv,f}$ [mmHgs/mL]	$R_{av,b}$ [mmHgs/mL]
NHVF	0.0025	-	-
$MV_{reg,mi}$	0.0025	0.3	-
$MV_{reg,mo}$	0.0025	0.1	-
$MV_{ste,mi}$	0.035	-	-
$MV_{ste,mo}$	0.090	-	-
$AV_{reg,mi}$	0.0025	-	1.5
$AV_{reg,mo}$	0.0025	-	3

NHVF, MV and AV are normal heart valve function, mitral and aortic valves, R is the resistance, subscripts reg, ste, mi and mo represent regurgitation, stenosis, mild and moderate, f and b represent forward and backward blood flow.

The main mechanical components of an axial flow CF-LVAD are an inducer, impeller, and diffuser in a flow channel. The rotating impeller accelerates the blood and generates blood flow whilst increasing the outlet pressure of the CF-LVAD to improve the perfusion level in the cardiovascular system. The motor stator located in the pump housing generates a magnetic field and magnets embedded impeller rotate the impeller. In this study, CF-LVAD electrical current waveform is used to monitor the changing conditions in a heart with CF-LVAD. An illustrated representation of a CF-LVAD-supported heart and the main electrical and mechanical components of the CF-LVAD together with studied clinical cases are given in Figure 1.

CF-LVAD was operated at 10000 rpm speed by using proportional-integral (PI) control which regulated the pump current in the simulations. P and I gains were 0.008338 and
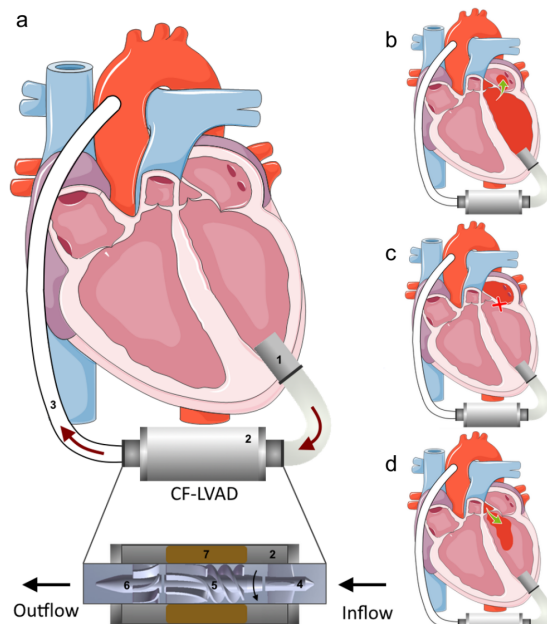

Fig. 1. Illustration of a failing left ventricle and CF-LVAD support. a) Inflow cannula (1) positioned at the left ventricular apex, pump housing (2) and the outflow graft (3) between the pump outlet and ascending aorta, inducer (4), impeller (5), diffuser (6) and motor stator (7) in the CF-LVAD, b) mitral regurgitation in a heart with CF-LVAD, c) mitral stenosis in a heart with CF-LVAD, d) aortic regurgitation in a heart with CF-LVAD.

4.007 respectively and they were tuned using the PID tuner application in Simulink. Simulations were performed in Matlab Simulink R2021b using variable step size ode15s solver. Maximum step size was 1e-3 s and relative tolerance was 1e-3 in all the simulations. The electric analogue of the cardiovascular system model is given Figure 2.
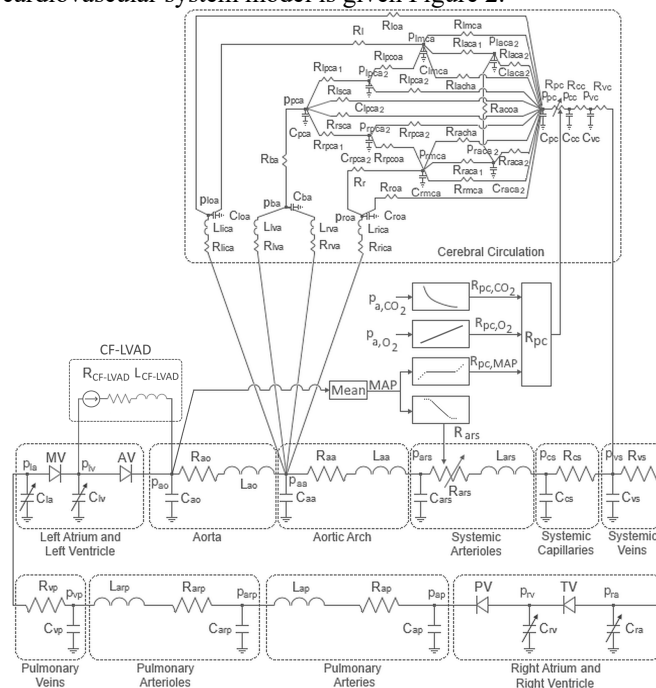

Fig. 2. Electric circuit representation of the cardiovascular system model with the CF-LVAD.

Skewness and kurtosis of CF-LVAD electrical current and flow rate signals waveforms over left ventricular systole and left atrial contraction were compared considering Gaussian curves. Because mitral and aortic blood flow occurs due to

This article has been accepted for publication in IEEE Sensors Journal. This is the author's version which has not been fully edited and
content may change prior to final publication. Citation information: DOI 10.1109/JSEN.2023.3292803

> REPLACE THIS LINE WITH YOUR PAPER IDENTIFICATION NUMBER (DOUBLE-CLICK HERE TO EDIT) <   4
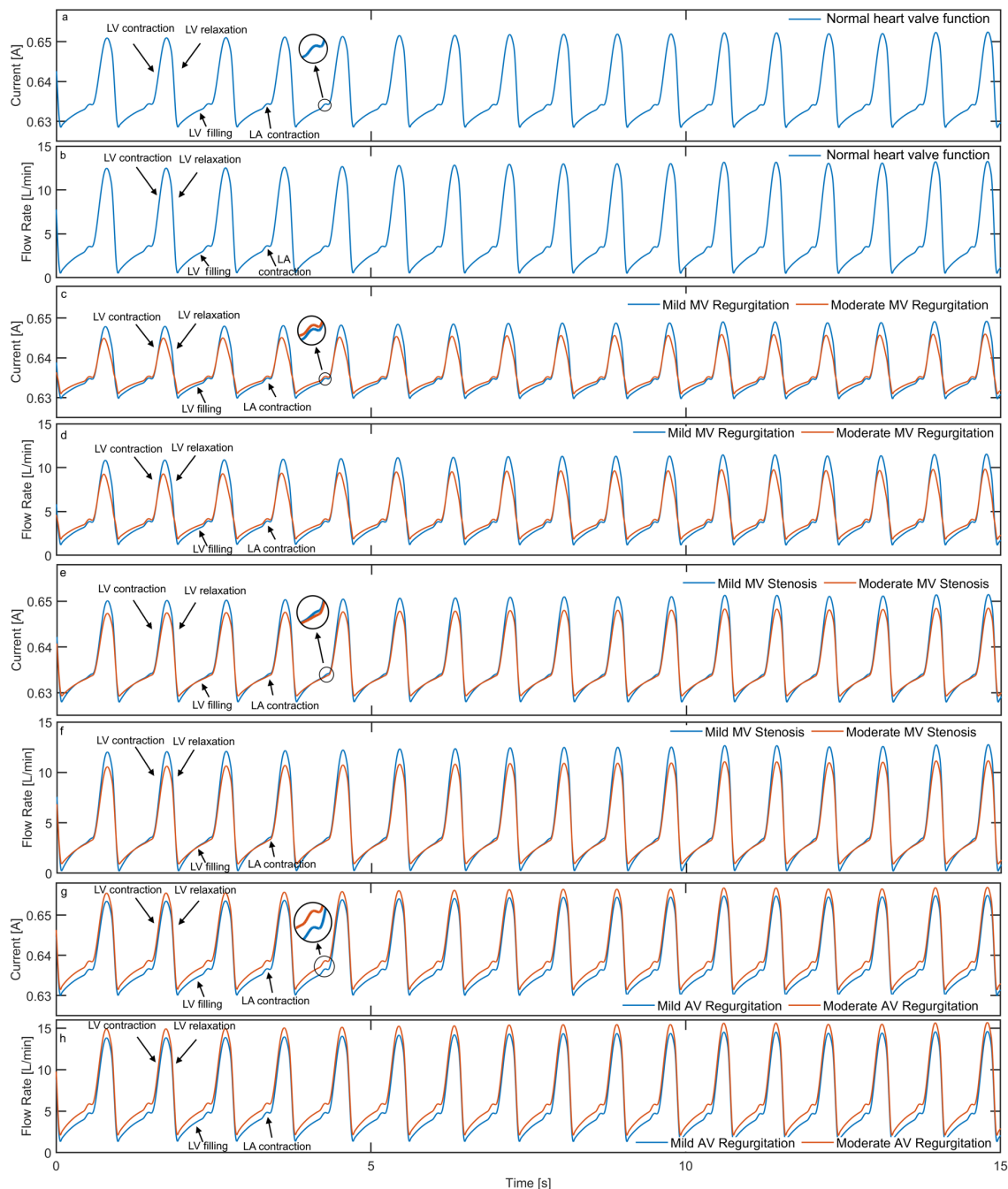
Fig. 3. a) CF-LVAD electrical current signal waveform, b) CF-LVAD flow rate signal waveform for normal heart valve function, c) CF-LVAD electrical current signal waveform, d) CF-LVAD flow rate signal waveform for mild and moderate mitral regurgitation, e) CF-LVAD electrical current signal waveform, f) CF-LVAD flow rate signal waveform for mild and moderate mitral stenosis, g) CF-LVAD electrical current signal waveform, h) CF-LVAD flow rate signal waveform for mild and moderate aortic regurgitation (LV, LA, MV and AV represent left ventricle, left atrium, mitral valve and aortic valve).

active atrial and ventricular contractions over these cardiac cycle phases. The correlation between the CF-LVAD electrical current and flow rate and the severity of the mitral and aortic valve disorders was evaluated using the non-parametric spearman rank correlation in GraphPad Prism software. Correlations between the CF-LVAD current and flow rate and the valvular disorders were estimated during atrial contraction and ventricular systole. CF-LVAD current and flow rate sample distributions over the atrial contraction and ventricular systolic phases were calculated by modelling signal waveforms in a Gaussian distribution. Detailed information about the statistical

comparison of the CF-LVAD electrical current and flow rate signal waveforms are given as Supplementary Material.

III. RESULTS

CF-LVAD electrical current and flow rate signal waveforms over 15 seconds for normal heart valve function, mild and moderate mitral regurgitation and stenosis and mild and moderate aortic regurgitation are given in Figure 3.

The increased blood flow rate through the CF-LVAD due to left ventricular contraction increases also the left ventricular CF-LVAD electrical current. CF-LVAD electrical current
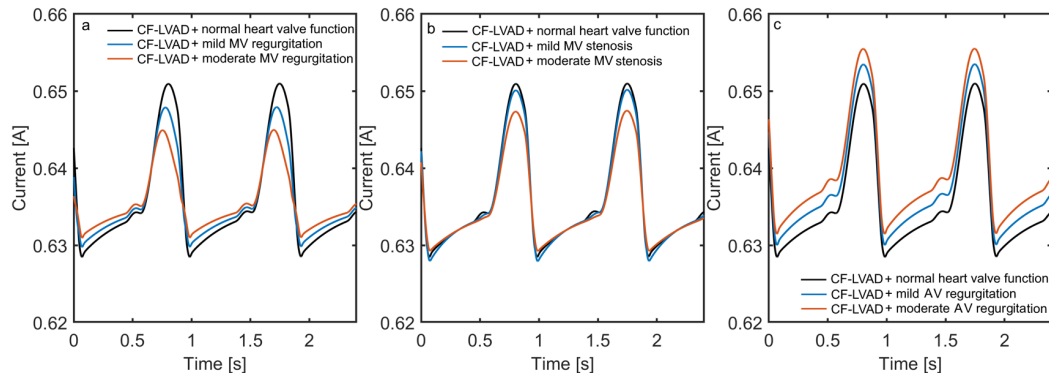
Fig. 4. CF-LVAD electrical current signal for a) normal heart valve function and mitral regurgitation, b) normal heart valve function and mitral stenosis, c) normal heart valve function and aortic regurgitation (MV and AV represent mitral valve and aortic valve).

decreases during the left ventricular relaxation because of the reduced CF-LVAD blood flow rate. CF-LVAD flow rate and electrical current increase during the left ventricular filling whereas a hump is noticeable CF-LVAD flow rate and electrical current signals dues to left atrial contraction. Mitral regurgitation altered CF-LVAD electrical current and flow rate signal waveforms over the left ventricular relaxation phase. Moreover, both amplitudes of the CF-LVAD electrical current and flow rate signals decreased with worsened mitral regurgitation. The hump due to left atrial contraction in CF-LVAD flow rate and electrical current signals was noticeable in mild and moderate regurgitation. Mitral stenosis reduced amplitudes of CF-LVAD flow rate and electrical current signals over a cardiac cycle. The hump due to left atrial contraction in CF-LVAD flow rate and electrical current signals disappeared in moderate mitral stenosis. Aortic regurgitation did not alter CF-LVAD flow rate and electrical current signals, however, both signals shifted up with worsened aortic regurgitation. Comparison of the CF-LVAD electrical signal waveforms for normal heart valve function and mitral regurgitation, mitral stenosis and aortic regurgitation is given in Figure 4.

Mitral regurgitation reduced the amplitude of CF-LVAD electrical current. Although left ventricular contraction did not affect the CF-LVAD electrical current signal waveform, maximal CF-LVAD electrical current over a cardiac cycle decreased with the worsening of the regurgitation through the mitral valve. Also, minimal CF-LVAD current over a cardiac cycle increased with worsening of mitral regurgitation. Mitral stenosis reduced maximal CF-LVAD current over a cardiac cycle. Worsened mitral stenosis resulted in a relatively higher reduction in maximal CF-LVAD electrical current over a cardiac cycle and CF-LVAD electrical current amplitude. Moreover, the stiffened mitral valve resulted in a relatively small hump in CF-LVAD electrical current signal in mild stenosis during atrial contraction and the hump in CF-LVAD electrical current signal disappeared in moderate mitral stenosis. Worsening of aortic regurgitation increased overall CF-LVAD electrical current over a cardiac cycle. Signal waveforms, skewness, and kurtosis of CF-LVAD electrical current and flow rate over left ventricular systole and left atrial contraction and the correlation between CF-LVAD electrical current and flow rate signal for normal heart valve function, mitral regurgitation, mitral stenosis, and aortic regurgitation are given in Figure 5.

CF-LVAD electrical current and flow rate signals over left

ventricular systole have negative skewness values for the simulated valvular conditions. Progress of the mitral regurgitation reduced the skewness of both CF-LVAD electrical current and flow rate signals over the left ventricular systole. Skewness of the CF-LVAD electrical current and flow rate signals over left ventricular systole in mild mitral stenosis was relatively high, however, worsened mitral stenosis reduced the skewness. Progress of the aortic regurgitation increased the skewness of the CF-LVAD electrical current and flow rate signals during the left ventricular systole. CF-LVAD electrical current signal over the left atrial contraction has negative skewness in the simulated valvular conditions apart from moderate aortic stenosis. Skewness of the CF-LVAD electrical current signal over the left atrial contraction in mild and moderate aortic stenosis was relatively less whereas other valvular conditions caused relatively high negative skewness in CF-LVAD electrical current signal during left atrial contraction. Skewness of the CF-LVAD flow rate signal during the left atrial contraction increased with the progression of mitral or aortic regurgitation. Although mild mitral stenosis results in a relatively less skewed CF-LVAD flow rate signal during left atrial contraction, the progression of mitral stenosis increases the skewness of the CF-LVAD flow rate signal during left atrial contraction.

Kurtoses of CF-LVAD electrical current signals over the left ventricular systole in simulated valvular conditions were comparable to each other as well as the CF-LVAD flow rate signals. Kurtoses of the CF-LVAD electrical current signals over the left atrial contraction were positive for normal valvular function, and mitral and aortic regurgitation whereas negative kurtosis values characterised mitral stenosis. On the other hand, CF-LVAD flow rate signal during left atrial contraction had positive kurtosis values. Mitral or aortic regurgitation increased kurtosis of the CF-LVAD flow rate signal during left atrial contraction. Although mild mitral stenosis results in a smaller kurtosis CF-LVAD flow rate signal during left atrial contraction, the progression of mitral stenosis increases the kurtosis of the CF-LVAD flow rate signal during left atrial contraction.

Aortic regurgitation increased the overall CF-LVAD electrical current and flow rate over a cardiac cycle, therefore, high negative differences in the mean values in these signals were obtained. Mitral stenosis decreased CF-LVAD electrical current and flow rate, therefore, positive differences in the mean values over left ventricular systolic and left atrial contraction
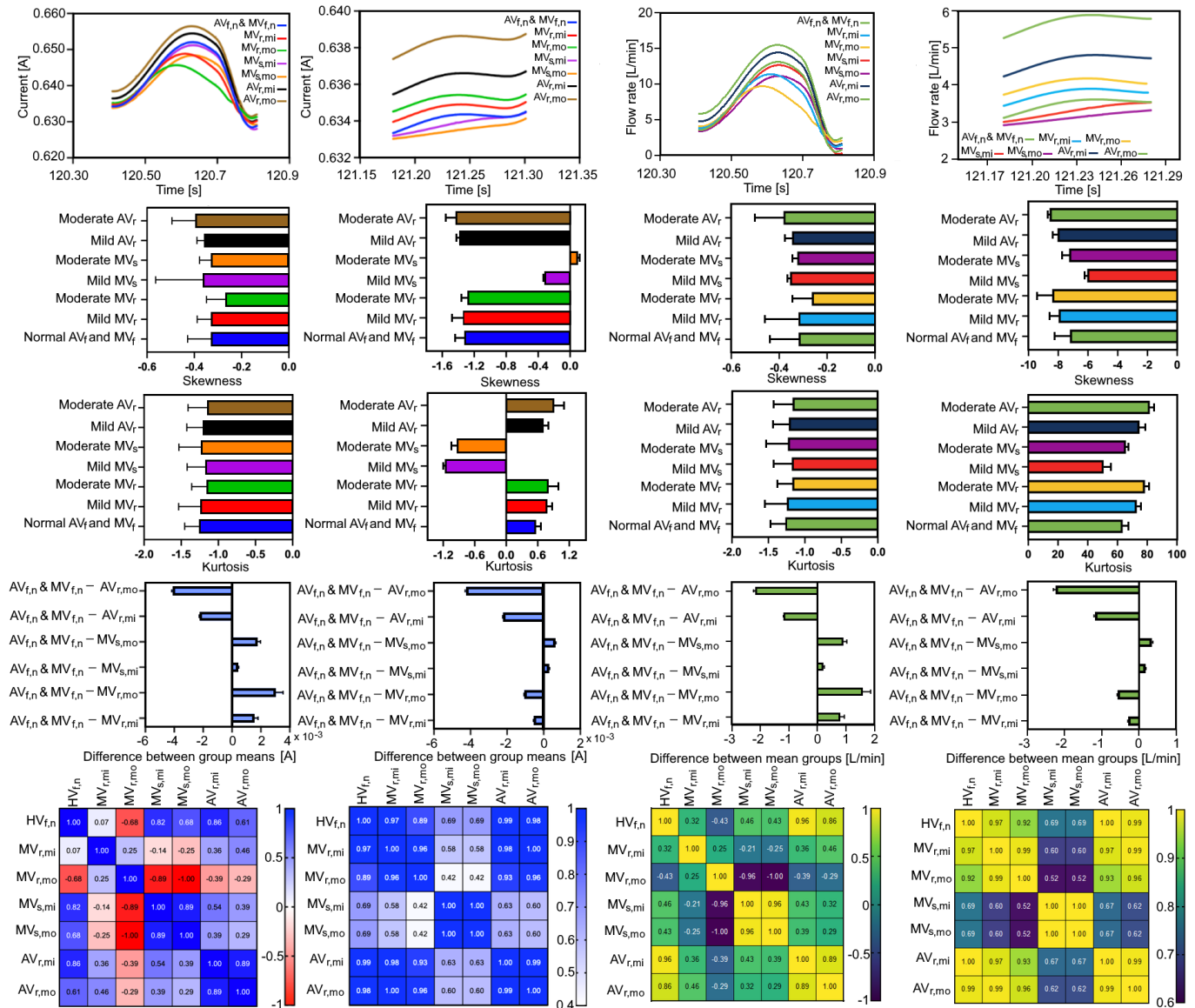
Fig. 5. Signal waveforms, skewness and kurtosis of CF-LVAD electrical current and flow rate over left ventricular systole and left atrial contraction for normal heart valve function, mitral regurgitation, mitral stenosis and aortic regurgitation, the correlation between CF-LVAD electrical current and flow rate signal over left ventricular systole and left atrial contraction for normal heart valve function, mitral regurgitation, mitral stenosis and aortic regurgitation (MV and AV represent mitral valve and aortic valve, subscripts f, n, mi, mo, r and, s represent function, normal, mild, moderate, regurgitation and stenosis).

phases in these signals were obtained. Mitral regurgitation decreased the CF-LVAD electrical current and flow rate during left ventricular systole and increased them during left atrial contraction. Therefore, differences in the mean groups were positive over left ventricular systole whereas differences in the mean groups were negative during left atrial contraction.

Spearman correlation revealed that mitral regurgitation affects CF-LVAD electrical current signal waveform during left ventricular systole. There was a low correlation ($\rho=0.07$) between the CF-LVAD electrical current signal waveforms in normal heart valve function and mild mitral regurgitation whereas the correlation was negative ($\rho=-0.68$) between the CF-LVAD electrical current signal waveforms in normal heart valve function and moderate mitral regurgitation. Although there was a high correlation ($\rho=0.82$) between the CF-LVAD electrical current signal waveforms in normal heart valve function and mild mitral stenosis, the progression of mitral

stenosis reduces the correlation coefficient ($\rho=0.68$) over left ventricular systole. Similarly, CF-LVAD electrical current signal waveforms in normal heart valve function and mild aortic regurgitation were highly correlated ($\rho=0.86$) whereas the progression of aortic regurgitation reduced the correlation coefficient ($\rho=0.61$) over left ventricular systole. CF-LVAD electrical current signal waveforms were in normal heart valve function and mitral and aortic regurgitation were highly correlated ($\rho=0.97, 0.89, 0.99$ and 0.98), whereas mitral stenosis reduced the correlation ($\rho=0.69$) between CF-LVAD electrical current signal waveforms in normal heart valve function and mitral stenosis during left atrial contraction.

IV. DISCUSSION

The amplitude of CF-LVAD electrical current and flow rate signal over a cardiac cycle reduced in mitral regurgitation. This was because reverse blood flow through the mitral valve during

left ventricular contraction and relaxation reduced forward CF-LVAD flow over left ventricular systole. CF-LVAD electrical current and flow rate signal waveforms were altered during left ventricular relaxation. Mitral regurgitation affects the relaxation function of the left ventricle because left atrial pressure and the left ventricular filling pressure at the beginning of left ventricular filling increase remarkably [32]. The correlation between CF-LVAD electrical signals in normal heart valve function and mild mitral regurgitation was extremely low whereas there was a negative correlation between CF-LVAD electrical signals in normal heart valve function and moderate mitral regurgitation over left ventricular systole. Such a result suggests that even mild mitral regurgitation can be detected from CF-LVAD electrical current and the progression of mitral regurgitation over time can be monitored.

Mitral stenosis affected CF-LVAD electrical current and flow rate signal waveforms during left atrial contraction. The amplitude of the hump in these signals due to atrial contraction decreased. Mitral valve leaflets thickened and immobile obstructing blood flow in mitral stenosis [33]. Therefore, increased left ventricular pressure because of atrial contraction is not noticeable in the left ventricle and CF-LVAD inlet pressure. The correlation coefficients between CF-LVAD electrical current signal in normal heart valve function and both mild and moderate mitral stenosis were 0.69 suggesting that mitral stenosis can be detected by monitoring CF-LVAD electrical current over left atrial contraction. Also, relatively low skewed CF-LVAD electrical current signals and negative kurtosis values may be used to detect mitral stenosis. However, monitoring CF-LVAD electrical current only over left atrial contraction or using skewness or kurtosis may not allow detection of the progression of mitral stenosis. The correlation coefficient for the CF-LVAD electrical current signal reduced from 0.82 to 0.68 for mild and moderate mitral stenosis over the left ventricular systole. Therefore, the progression of mitral stenosis can be detected by monitoring CF-LVAD current during both left ventricular systole and left atrial contraction.

CF-LVAD electrical current signals were highly correlated with each other for normal heart valve function and mild aortic regurgitation. The correlation coefficient between the CF-LVAD electrical current signals for normal heart valve function and moderate aortic regurgitation reduced to 0.61 over left ventricular systole. Therefore, moderate aortic regurgitation may be detected by comparing CF-LVAD electrical current signals over left ventricular systole. However, the detection of mild aortic regurgitation requires using a different method during CF-LVAD support.

The pump characteristics are expected to affect the results, however, problems in mitral and aortic valvular functions again will alter the electrical current signal waveforms and it will be possible to detect the altered signal waveforms. Therefore, the proposed methods to monitor the valvular functions can also be used in the third generation centrifugal CF-LVADs as well. Complications such as thrombosis may also affect the results and it may alter the signal waveforms further in a CF-LVAD. However, it is also possible to detect obstruction in a CF-LVAD

[34]. Therefore, again the proposed method can be utilised to detect and identify additional complications and it may be possible to monitor valvular functions in combination with the occurring complications in the patients implanted with CF-LVAD.

Monitoring mitral and aortic valvular function and detecting the severity of heart valve disorders in a cardiovascular system supported by a CF-LVAD without using additional sensors will help to avoid complications that may occur due to interaction with blood. Moreover, continuous monitoring and storing of data about the status of the heart during CF-LVAD support may be combined with the Internet of Things as described by [35] or smart biosensing technologies and portable devices with the transition Healthcare systems [36] will have a positive impact on patients' life quality.

In this study, severe mitral and aortic valve disorders were not studied because the aim was to show that it is possible to detect early-stage mitral and aortic valve disorders and monitor progression using CF-LVAD intrinsic parameters. Detection of moderate valvular disorders will reduce the risk of severe valvular disorders during CF-LVAD support. Also, aortic stenosis during CF-LVAD support was not studied in this paper because CF-LVAD support does not depend on the aortic valve function if the aortic valve remains closed over a cardiac cycle [37]. Cardiac phases must be detected to implement the proposed heart valve disorder monitoring method during CF-VAD support. CF-LVAD characteristics and electrical current waveform have been used to track the cardiac contractile state [38]. Similar methods can be used also to detect cardiac phases and the proposed method in this study can be used to monitor valvular function during CF-LVAD support.

V. Conclusion

In this work, CF-LVAD electrical current signal waveforms were monitored to detect mitral aortic valvular functions during CF-LVAD support. CF-LVAD electrical current signal waveforms can be used to evaluate the severity and progress of mitral and aortic disorders. This helps translate the measurands of a biodevice into biosensing signals without an additional physical element acting as a sensor in the feedback loop of the biodevice. These positive outcomes of our study have demonstrated the potential of conducting a sensor-free biosensing for CF-LVADs. The clinical translation of our study may lead to better monitoring of CF-LVAD patients and subsequently reduce morbidity and improve life quality of patients during CF-LVAD treatment.

References

[1] M. Mihalj *et al.*, "Third generation continuous flow left ventricular assist devices; a comparative outcome analysis by device type," *Eur. Heart J.*, vol. 42, no. Supplement_1, p. ehab724.0946, Oct. 2021, doi: 10.1093/eurheartj/ehab724.0946.

[2] N. McNamara *et al.*, "Contemporary outcomes of continuous-flow left ventricular assist devices—a systematic review," *Ann. Cardiothorac. Surg.*, vol. 10, no. 2, Art. no. 2, Mar. 2021, doi: 10.21037/acs-2021-cfmcs-35.

[3] P.-E. Noly *et al.*, "Continuous-Flow Left Ventricular Assist Devices and Valvular Heart Disease: A Comprehensive Review," *Can. J.*

This article has been accepted for publication in IEEE Sensors Journal. This is the author's version which has not been fully edited and content may change prior to final publication. Citation information: DOI 10.1109/JSEN.2023.3292803

> REPLACE THIS LINE WITH YOUR PAPER IDENTIFICATION NUMBER (DOUBLE-CLICK HERE TO EDIT) <   8

Cardiol., vol. 36, no. 2, pp. 244–260, Feb. 2020, doi: 10.1016/j.cjca.2019.11.022.

[4] C. Maxwell and G. Whitener, "Mitral Intervention with LVAD: Preparing for Recovery," *Semin. Cardiothorac. Vasc. Anesth.*, vol. 23, no. 1, pp. 134–139, Mar. 2019, doi: 10.1177/1089253218788081.

[5] S. Rosenkranz, J. S. R. Gibbs, R. Wachter, T. De Marco, A. Vonk-Noordegraaf, and J.-L. Vachiéry, "Left ventricular heart failure and pulmonary hypertension," *Eur. Heart J.*, vol. 37, no. 12, pp. 942–954, Mar. 2016, doi: 10.1093/eurheartj/ehv512.

[6] S. Taghavi *et al.*, "Mitral valve repair at the time of continuous-flow left ventricular assist device implantation confers meaningful decrement in pulmonary vascular resistance," *ASAIO J. Am. Soc. Artif. Intern. Organs 1992*, vol. 59, no. 5, pp. 469–473, 2013, doi: 10.1097/MAT.0b013e31829be026.

[7] R. L. Kormos *et al.*, "Right ventricular failure in patients with the HeartMate II continuous-flow left ventricular assist device: incidence, risk factors, and effect on outcomes," *J. Thorac. Cardiovasc. Surg.*, vol. 139, no. 5, pp. 1316–1324, May 2010, doi: 10.1016/j.jtcvs.2009.11.020.

[8] P.-E. Noly *et al.*, "Role of the mitral valve in left ventricular assist device pathophysiology," *Front. Cardiovasc. Med.*, vol. 9, 2022, Accessed: Dec. 02, 2022. [Online]. Available: https://www.frontiersin.org/articles/10.3389/fcvm.2022.1018295

[9] A. Pawale, S. Itagaki, A. Parikh, S. P. Pinney, D. H. Adams, and A. C. Anyanwu, "Mitral valve repair for severe mitral valve regurgitation during left ventricular assist device implantation," *J. Thorac. Cardiovasc. Surg.*, vol. 157, no. 5, pp. 1841-1848.e1, May 2019, doi: 10.1016/j.jtcvs.2018.12.071.

[10] H. Baumgartner *et al.*, "Echocardiographic assessment of valve stenosis: EAE/ASE recommendations for clinical practice," *Eur. J. Echocardiogr. J. Work. Group Echocardiogr. Eur. Soc. Cardiol.*, vol. 10, no. 1, pp. 1–25, Jan. 2009, doi: 10.1093/ejechocard/jen303.

[11] E. Tuzun *et al.*, "Assessment of aortic valve pressure overload and leaflet functions in an ex vivo beating heart loaded with a continuous flow cardiac assist device," *Eur. J. Cardiothorac. Surg.*, vol. 45, no. 2, pp. 377–383, Feb. 2014, doi: 10.1093/ejcts/ezt355.

[12] E. J. Farrar, G. D. Huntley, and J. Butcher, "Endothelial-derived oxidative stress drives myofibroblastic activation and calcification of the aortic valve," *PloS One*, vol. 10, no. 4, p. e0123257, 2015, doi: 10.1371/journal.pone.0123257.

[13] Y. Tanaka *et al.*, "The impact of uncorrected mild aortic insufficiency at the time of left ventricular assist device implantation," *J. Thorac. Cardiovasc. Surg.*, vol. 160, no. 6, pp. 1490-1500.e3, Dec. 2020, doi: 10.1016/j.jtcvs.2020.02.144.

[14] D. V. Telyshev *et al.*, "Correlation between Myocardial Function and Electric Current Pulsatility of the Sputnik Left Ventricular Assist Device: In-Vitro Study," *Appl. Sci.*, vol. 11, no. 8, Art. no. 8, Jan. 2021, doi: 10.3390/app11083359.

[15] M. Fetanat, M. Stevens, C. Hayward, and N. H. Lovell, "A Sensorless Control System for an Implantable Heart Pump Using a Real-Time Deep Convolutional Neural Network," *IEEE Trans. Biomed. Eng.*, vol. 68, no. 10, pp. 3029–3038, Oct. 2021, doi: 10.1109/TBME.2021.3061405.

[16] M. Maw *et al.*, "A Sensorless Modular Multiobjective Control Algorithm for Left Ventricular Assist Devices: A Clinical Pilot Study," *Front. Cardiovasc. Med.*, vol. 9, 2022, Accessed: Feb. 25, 2023. [Online]. Available: https://www.frontiersin.org/articles/10.3389/fcvm.2022.888269

[17] L. Hubbert, J. Baranowski, B. Delshad, and H. Ahn, "Left Atrial Pressure Monitoring With an Implantable Wireless Pressure Sensor After Implantation of a Left Ventricular Assist Device," *Asaio J.*, vol. 63, no. 5, pp. e60–e65, Sep. 2017, doi: 10.1097/MAT.0000000000000451.

[18] M.-D. Zhou, C. Yang, Z. Liu, J. P. Cysyk, and S.-Y. Zheng, "An implantable Fabry-Pérot pressure sensor fabricated on left ventricular assist device for heart failure," *Biomed. Microdevices*, vol. 14, no. 1, pp. 235–245, Feb. 2012, doi: 10.1007/s10544-011-9601-z.

[19] S. Staufert and C. Hierold, "Novel Sensor Integration Approach for Blood Pressure Sensing in Ventricular Assist Devices," *Procedia Eng.*, vol. 168, pp. 71–75, Jan. 2016, doi: 10.1016/j.proeng.2016.11.150.

[20] A. F. Stephens, A. Busch, R. F. Salamonsen, S. D. Gregory, and G. D. Tansley, "A novel fibre Bragg grating pressure sensor for rotary ventricular assist devices," *Sens. Actuators Phys.*, vol. 295, pp. 474–482, Aug. 2019, doi: 10.1016/j.sna.2019.06.028.

[21] I. Tchoukina, M. C. Smallfield, and K. B. Shah, "Device Management and Flow Optimization on Left Ventricular Assist Device Support," *Crit. Care Clin.*, vol. 34, no. 3, pp. 453–463, Jul. 2018, doi: 10.1016/j.ccc.2018.03.002.

[22] A. L. Goldberger *et al.*, "PhysioBank, PhysioToolkit, and PhysioNet: components of a new research resource for complex physiologic signals," *Circulation*, vol. 101, no. 23, pp. E215-220, Jun. 2000.

[23] P. Lancellotti *et al.*, "European Association of Echocardiography recommendations for the assessment of valvular regurgitation. Part 2: mitral and tricuspid regurgitation (native valve disease)," *Eur. J. Echocardiogr.*, vol. 11, no. 4, pp. 307–332, May 2010, doi: 10.1093/ejechocard/jeq031.

[24] G. Ganesan, "How to assess mitral stenosis by echo - A step-by-step approach," *J. Indian Acad. Echocardiogr. Cardiovasc. Imaging*, vol. 1, no. 3, pp. 197–205, Dec. 2017, doi: 10.4103/jiae.jiae_38_17.

[25] P. Lancellotti *et al.*, "European Association of Echocardiography recommendations for the assessment of valvular regurgitation. Part 1: aortic and pulmonary regurgitation (native valve disease)," *Eur. J. Echocardiogr.*, vol. 11, no. 3, pp. 223–244, Apr. 2010, doi: 10.1093/ejechocard/jeq030.

[26] W. L. Holman, "Interagency Registry for Mechanically Assisted Circulatory Support (INTERMACS): what have we learned and what will we learn?," *Circulation*, vol. 126, no. 11, pp. 1401–1406, Sep. 2012, doi: 10.1161/CIRCULATIONAHA.112.097816.

[27] S. Bozkurt, A. Volkan Yilmaz, K. Bakaya, A. Bharadwaj, and K. K. Safak, "A novel computational model for cerebral blood flow rate control mechanisms to evaluate physiological cases," *Biomed. Signal Process. Control*, vol. 78, p. 103851, Sep. 2022, doi: 10.1016/j.bspc.2022.103851.

[28] S. Bozkurt, "Mathematical modeling of cardiac function to evaluate clinical cases in adults and children," *PloS One*, vol. 14, no. 10, p. e0224663, 2019, doi: 10.1371/journal.pone.0224663.

[29] E. Sorguven *et al.*, "Flow Simulation and Optimization of a Left Ventricular Assist Device," presented at the ASME 2007 International Mechanical Engineering Congress and Exposition, American Society of Mechanical Engineers Digital Collection, May 2009, pp. 1401–1407. doi: 10.1115/IMECE2007-41747.

[30] S. Bozkurt and S. Bozkurt, "In-silico evaluation of left ventricular unloading under varying speed continuous flow left ventricular assist device support," *Biocybern. Biomed. Eng.*, vol. 37, no. 3, pp. 373–387, Jan. 2017, doi: 10.1016/j.bbe.2017.03.003.

[31] S. Bozkurt, "Dynamic Modeling of Human Cardiovascular System and an Axial Heart Pump," Masters, Yeditepe University, 2009. Accessed: Oct. 20, 2022. [Online]. Available: https://discovery.ucl.ac.uk/id/eprint/1461003/

[32] H. Patel, M. Desai, E. M. Tuzcu, B. Griffin, and S. Kapadia, "Pulmonary Hypertension in Mitral Regurgitation," *J. Am. Heart Assoc.*, vol. 3, no. 4, p. e000748, 2014, doi: 10.1161/JAHA.113.000748.

[33] A. S. Omran, A. A. Arifi, and A. A. Mohamed, "Echocardiography in mitral stenosis," *J. Saudi Heart Assoc.*, vol. 23, no. 1, pp. 51–58, Jan. 2011, doi: 10.1016/j.jsha.2010.07.007.

[34] D. Lilja, I. Schalit, A. Espinoza, F.-J. Pettersen, O. J. Elle, and P. S. Halvorsen, "Detection of inflow obstruction in left ventricular assist devices by accelerometer: An in vitro study," *Med. Eng. Phys.*, vol. 110, p. 103917, Dec. 2022, doi: 10.1016/j.medengphy.2022.103917.

[35] J. T. Kelly, K. L. Campbell, E. Gong, and P. Scuffham, "The Internet of Things: Impact and Implications for Health Care Delivery," *J. Med. Internet Res.*, vol. 22, no. 11, p. e20135, Nov. 2020, doi: 10.2196/20135.

[36] T. Naghdi, S. Ardalan, Z. Asghari Adib, A. R. Sharifi, and H. Golmohammadi, "Moving toward smart biomedical sensing," *Biosens. Bioelectron.*, vol. 223, p. 115009, Mar. 2023, doi: 10.1016/j.bios.2022.115009.

[37] T. S. Wang, A. F. Hernandez, G. M. Felker, C. A. Milano, J. G. Rogers, and C. B. Patel, "Valvular Heart Disease in Patients Supported With Left Ventricular Assist Devices," *Circ. Heart Fail.*, vol. 7, no. 1, pp. 215–222, Jan. 2014, doi: 10.1161/CIRCHEARTFAILURE.113.000473.

[38] B. Y. Chang, Z. Zhang, K. Feng, N. Josephy, S. P. Keller, and E. R. Edelman, "Hysteretic device characteristics indicate cardiac contractile state for guiding mechanical circulatory support device use," *Intensive Care Med. Exp.*, vol. 9, no. 1, p. 62, Dec. 2021, doi: 10.1186/s40635-021-00426-3.